J|A|C|S
ARTICLES
Published on Web 07/09/2002

# Mechanism of Ruthenium-Catalyzed Olefin Metathesis Reactions from a Theoretical Perspective

Luigi Cavallo*

*Contribution from the Dipartimento di Chimica, Università di Salerno, Via Salvador Allende, Baronissi, Salerno I-84081, Italy*

Received August 6, 2001

***Abstract:*** This paper presents a density functional theory study of the ruthenium-catalyzed olefin metathesis reactions. The ligand binding energy has been calculated in the first generation of Grubbs-type $(PCy_3)_2Cl_2Ru{=}CHPh$ (pre)catalyst, as well as in the heteroleptic (pre)catalytic systems in which a *N*-heterocyclic carbene, NHC, ligand substitutes a single phosphine. In agreement with experiments $PCy_3$ coordinates more strongly to Ru in the heteroleptic (pre)catalysts than in the Grubbs-type (pre)catalyst. Moreover, ethene coordination and insertion into the Ru−alkylidene bond in the above-mentioned systems, as well as in the Hofmann type catalytic system with a *cis*-coordinated phosphane ligand, has been studied. The calculated insertion barrier for the NHC systems are lower than that of the $(PCy_3)_2Cl_2Ru{=}CHPh$ system. This is consistent with the higher activity experimentally observed for the NHC-based system.

## Introduction

The area of ruthenium-catalyzed olefin metathesis reactions is a remarkable topic in current chemistry because of its relevance as an efficient and elegant method to form C=C double bonds.[1−4] The discovery by Grubbs and co-workers of well-defined Ru-based (pre)catalysts, such as $(PCy_3)_2Cl_2Ru{=}CHPh$,[5] broadened its scope significantly, because they operate in mild conditions and are highly tolerant toward heteroatom-containing functional groups. Recently, substitution of a single phosphine by a *N*-heterocyclic carbene, NHC, ligand led to heteroleptic (pre)catalysts whose activity is not only higher than that of the "classical" $(PCy_3)_2Cl_2Ru{=}CHPh$ catalyst, but rivals that of early transition-metal catalysts.[6−9] The discovery by Hofmann and co-workers of Ru complexes with chelating bisphosphane ligands[10,11] and by Fürstner and co-workers of cationic allenylidene Ru complexes[12] opened new routes. Tuning and new uses of this reaction contribute to its relevance as an effective tool in organometallic chemistry.[13−20]

***Scheme 1***

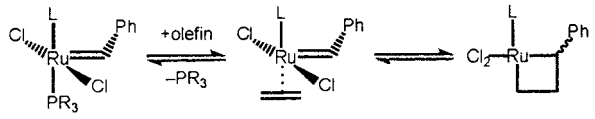


Experimental[21−25] and theoretical[23,26] studies converged to the mechanism briefly reported in Scheme 1 as the most probable. Substitution of a phosphine from the starting complex by the olefinic substrate generates the 16-electron intermediate in which the olefin is cis coordinated to the alkylidene. Reaction of the olefin with the alkylidene moiety, then, leads to the metallacycle intermediate that rapidly evolves toward products.

The formation of the phosphine-dissociated but olefin-bound intermediate is supported by kinetic data,[21] isolation and characterization of a monophosphine Ru catalyst "caught in the act",[27] detection of monophosphine intermediates by electrospray ionization tandem mass spectrometry,[23,28] and quantum mechan-

* Corresponding author E-mail address: lcavallo@unisa.it.

(1) Ivin, K. J.; Mol, J. C. *Olefin Metathesis and Metathesis Polymerization*; Academic Press: San Diego, CA, 1997.
(2) Fürstner, A. *Angew. Chem., Int. Ed.* **2000**, *39*, 3012.
(3) Buchmeiser, M. R. *Chem. Rev.* **2000**, *100*, 1565.
(4) Trnka, T. M.; Grubbs, R. H. *Acc. Chem. Res.* **2001**, *34*, 18.
(5) Nguyen, S. T.; Grubbs, R. H.; Ziller, J. W. *J. Am. Chem. Soc.* **1993**, *115*, 9858.
(6) Scholl, M.; Ding, S.; Lee, C. W.; Grubbs, R. H. *Org. Lett.* **1999**, *1*, 953.
(7) Huang, J.; Stevens, E. D.; Nolan, S. P.; Peterson, J. L. *J. Am. Chem. Soc.* **1999**, *121*, 2674.
(8) Weskamp, T.; Kohl, F. J.; Hieringer, W.; Gleich, D.; Herrmann, W. A. *Angew. Chem., Int. Ed. Engl.* **1999**, *38*, 2416.
(9) Bielawski, C. W.; Grubbs, R. H. *Angew. Chem., Int. Ed.* **2000**, *39*, 2903.
(10) Hansen, S. M.; Volland, M. A. O.; Rominger, F.; Eisenträger, F.; Hofmann, P. *Angew. Chem., Int. Ed. Engl.* **1999**, *38*, 1273.
(11) Hansen, S. M.; Rominger, F.; Metz, M.; Hofmann, P. *Chem. Eur. J.* **1999**, *5*, 557.
(12) Fürstner, A.; Liebl, M.; Lehmann, C. W.; Picquet, M.; Kunz, R.; Bruneau, C.; Touchard, D.; Dixneuf, P. H. *Chem. Eur. J.* **2000**, *6*, 1847.
(13) Fürstner, A.; Ackermann, L.; Gabor, B.; Goddard, R.; Lehmann, C. W.; Mynott, R.; Stelzer, F.; Thiel, O. R. *Chem. Eur. J.* **2001**, *7*, 3236.
(14) La, D. S.; Sattely, E. S.; Ford, J. G.; Schrock, R. R.; Hoveyda, A. H. *J. Am. Chem. Soc.* **2001**, *123*, 7767.
(15) Louie, J.; Bielawski, C. W.; Grubbs, R. H. *J. Am. Chem. Soc.* **2001**, *123*, 11312.
(16) Kouie, J.; Grubbs, R. H. *Angew. Chem., Int. Ed.* **2001**, *40*, 247.
(17) Choi, T.-L.; Woo Lee, C.; Chatterjee, A. K.; Grubbs, R. H. *J. Am. Chem. Soc.* **2001**, *123*, 10417.
(18) Fürstner, A.; Ackermann, L.; Beck, K.; Hori, H.; Koch, D.; Langemann, K.; Liebl, M.; Six, C.; Leitner, W. *J. Am. Chem. Soc.* **2001**, *123*, 9000.
(19) Liu, L.; Postema, M. H. D. *J. Am. Chem. Soc.* **2001**, *123*, 8602.
(20) Choi, T.-L.; Chatterjee, A. K.; Grubbs, R. H. *Angew. Chem., Int. Ed.* **2001**, *40*, 1277.
(21) Dias, E. L.; Nguyen, S. T.; Grubbs, R. H. *J. Am. Chem. Soc.* **1997**, *119*, 3887.
(22) Ulman, M.; Grubbs, R. H. *Organometallics* **1998**, *17*, 2484.
(23) Adlhart, C.; Hinderling, C.; Baumann, H.; Chen, P. *J. Am. Chem. Soc.* **2000**, *122*, 8204.
(24) Adlhart, C.; Volland, M. A. O.; Hofmann, P.; Chen, P. *Helv. Chim. Acta* **2000**, *83*, 3306.
(25) Adlhart, C.; Chen, P. *Helv. Chim. Acta* **2000**, *83*, 2192.
(26) Aagaard, O. M.; Meier, R. J.; Buda, F. *J. Am. Chem. Soc.* **1998**, *120*, 7174.
(27) Tallarico, J. A.; Bonitatebus, P. J., Jr.; Snapper, M. L. *J. Am. Chem. Soc.* **1997**, *119*, 7157.

***Scheme 2***

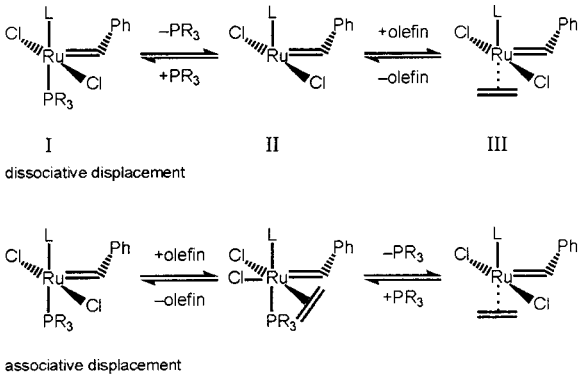


***Chart 1***

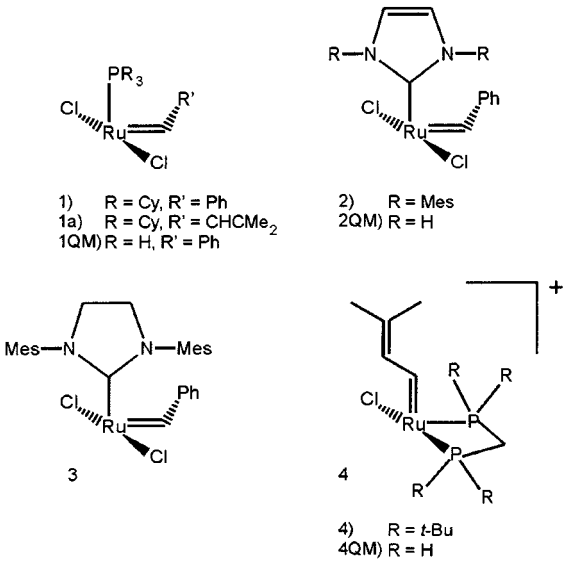


ics studies.[8,23,25,26] The formation of this intermediate can occur according to the mechanisms sketched in Scheme 2.

In the former, dissociation of the phosphine from **I** does not require precoordination of the olefin, and leads to the 14-electron intermediate **II** that can coordinate the olefin. The associative mechanism, instead, requires formation of an octahedral intermediate. Recent multitechnique experimental results of Grubbs and co-workers on the mechanism of metathesis reactions[29,30] were particularly informative since they clearly indicated that (1) the mechanism of dissociative displacement is favored and (2) a phosphine such as $PCy_3$ binds more strongly to Ru in the NHC-based systems than in the "classical" (pre)system with two $PCy_3$ bonded to Ru. Additionally, they gave a measure of this preference;[30] (3) the relative propensity of the naked intermediate **II** to be trapped back by the phosphine, or to coordinate the olefin to give the metathesis reaction, is one of the keys to understanding the relative activity of different catalysts. In short, they suggested that the slower initiation rate of the NHC-based (pre)catalysts relative to the "classical" (pre)-catalysts is a consequence of the higher binding energy of the leaving $PR_3$ group, while their higher catalytic activity is related to their higher propensity to coordinate the olefinic substrate.

Almost at the same time, Hofmann, Chen, and co-workers reported on an elegant comparison of the gas-phase and solution-phase intrinsic olefin metathesis rates shown by $(PCy_3)_2Cl_2$-Ru=CHPh and Hofmann- type $\{[(t\text{-}Bu)_2P(CH_2)P(t\text{-}Bu)_2](Cl)$-$Ru{=}CH{-}CH{=}C(CH_3)_2\}^+$ systems.[24] Their results established that the intrinsic gas-phase reactivity of the Grubbs-type catalysts is roughly 40 times higher than that of the Hofmann-type, and that the reverse occurs in solution. These results indicated that the higher activity of the Hofmann-type systems in solution is due to a more favorable activation step, rather than to higher intrinsic reactivity in the metathesis step. Finally, on the basis of kinetic isotope effects Chen and co-workers suggested that the metallacycle of Scheme 1 is a transition state rather than an intermediate.[23]

While the experimental mechanistic understanding of this class of reactions advanced with an impressive pace, only a few theoretical studies have been performed on the subject.[8,10,11,23,26,31,32]

In a first ab initio molecular dynamic study on the simple $(PH_3)_2Ru{=}CH_2$ model, Meier and co-workers found that dissociation of one of the phosphines was facile, and would lead to an active species.[26] This was in good qualitative agreement with prior experimental studies, which established that phosphine dissociation was indeed mandatory to achieve high catalytic activity.[21] Subsequently, Hofmann and co-workers performed a study of model compounds with *cis*- and *trans*-phosphane ligands, as a preliminary analysis to the synthesis of diphosphanylmethane complexes, and concluded that a small bite angle was needed to achieve a relative cis geometry of the coordinating P atoms.[10] They also investigated the successive metathesis reaction.[31] A detailed study of the complete reaction profile (from the bisphosphane (pre)catalyst to the metallacycle) was performed by Chen and co-workers.[23] Using the simple $(PH_3)_2$-$Ru{=}CH_2$ model, they gave a first estimate of the energy required to dissociate one of the phosphines, the olefin uptake energy, and the energy barrier for the metathesis reaction. Herrmann and co-workers performed the first comparison between different catalysts, since they calculated the binding energy of the different ligands in bisphosphanes and heteroleptic (pre)catalysts with NHC ligands.[8] In agreement with experiments, they found that the NHC ligands have a higher binding energy than phosphane ligands, and the binding energies they calculated are in valuable quantitative agreement with the experimental data.[30]

Although all these studies provided insight into the mechanism of olefin metathesis, they used simple models, which are extremely valuable to understanding the basic electronic features of the reaction mechanism, but lack the steric and electronic effects of real catalytic systems. In the wake of these seminal studies, and with the aim to contribute to reduce the gap between experiments and theory, we here report on a quantum mechanics study of olefin metathesis reactions with the olefin-free structures **II** sketched in Chart 1.

System **1** was discovered by Grubbs and it is the prototype of this class of catalysts.[5] It is a benchmark for both experimentalists and theoreticians. Systems **2** and **3**, also discovered by Grubbs, correspond to the NHC-based catalysts[6−9] and differ for the presence of a C=C double bond in the imidazolyl ring

(28) Hinderling, C.; Adlhart, C.; Baumann, H.; Chen, P. *Angew. Chem., Int. Ed. Engl.* **1998**, *37*, 7.
(29) Sanford, M. S.; Ulman, M.; Grubbs, R. H. *J. Am. Chem. Soc.* **2001**, *123*, 749.
(30) Sanford, M. S.; Love, J. A.; Grubbs, R. H. *J. Am. Chem. Soc.* **2001**, *123*, 6543.
(31) Volland, M. A.; Hansen, S. M.; Hofmann, P. *Chemistry at the Beginning of the Third Millennium*; Fabbrizzi, L., Poggi, A., Eds.; Springer: Berlin, Germany, 2000; p 23.

of **2**. Experimentally, systems similar to **2** were shown to have slightly lower activation parameters for phosphine exchange, and to be more active in the polymerization of cyclooctadiene, than systems similar to **3**.[30] A rationalization of these experimental differences represents a good test for any computational approach, due to the similarity between **2** and **3**. Finally, system **4** was discovered by Hofmann and it is an example of the recently introduced cationic bisphosphine-based systems.[10,11] Chen, Hofmann, and co-workers experimentally compared these new cationic systems and the first generation of Grubbs systems.[24] For this reason, a theoretical comparison between them is certainly useful.

For systems **1**−**3** we investigated phosphine dissociation, which can be considered to correspond to the activation step, according to the dissociative mechanism of Scheme 2, and as established by experimental studies.[29,30] This part can be considered as a calibration of the computational approach used, and will furnish a theoretical framework to the already self-consistent experimental data.

In the second part, we will report on the metathesis reaction composed of the olefin-coordination step (with ethene as probe olefin) followed by formation of the metallacycle. The primary scope of this part is to furnish details on the mechanism of the metathesis step. Finally, by considering suitable simplified models we will try to shed light on the role of the Cy, Mes, and *t*-Bu groups in metathesis reactions.

For the sake of readability, we will use the following notation. To denote the phosphine- and the ethene-bound intermediates **I** and **III**, we will use labels such as **1**·$PCy_3$ or **2**·$C_2H_4$, which correspond to the intermediates **I** and **III** obtained by coordination of $PCy_3$ and $C_2H_4$ to **1** and **2**, respectively. To denote the transition states which connect the olefin-bound intermediate to the metallacycle and the metallacycles obtained as products of the metathesis step, we will use labels such as **1**·TS and **2**·Mcy.

All the geometries herewith reported have been obtained with the pure BP86 density functional. The performance of this model in reproducing geometries of organometallic compounds and energetics of reactions[33−35] is witnessed by several studies on transition-metal-catalyzed reactions as the olefin polymerizations with early[36−39] and late[40,41] transition metals, olefin hydroformylation Co and Rh catalyzed,[42,43] methyl carbonylation Rh catalyzed,[44,45] and olefin epoxidation with Mn-salen catalysts.[46,47] Due to the size of the systems considered here, a different quantum mechanics approach in the geometry optimizations would have been almost prohibitive.

## Computational Details

Stationary points on the potential energy surface were calculated with the Amsterdam Density Functional (ADF) program.[48−51] The electronic configuration of the molecular systems was described by a triple-ζ STO basis set on ruthenium for 4s, 4p, 4d, 5s, 5p (ADF basis set IV). Double-ζ STO basis sets were used for phosphorus and chlorine (3s,3p), nitrogen and carbon (2s,2p), and hydrogen (1s), augmented with a single 3d, 3d, and 2p function, respectively (ADF basis set III).[48] The inner shells on ruthenium (including 3d), phosphorus and chlorine (including 2p), and nitrogen and carbon (1s) were treated within the frozen core approximation. Energies and geometries were evaluated by using the local exchange-correlation potential by Vosko et al.,[52] augmented in a self-consistent manner with Becke's[53] exchange gradient correction and Perdew's[54,55] correlation gradient correction.

The minima were localized by full optimization of the starting structures. The convergence criterions in the geometry optimizations were set to $7.5 \times 10^{-4}$ and $5 \times 10^{-4}$ au on the maximum and root-mean-square Cartesian gradients. Transition states were approached through a linear transit procedure, which started from the ethene-bound coordinated intermediates and terminated at the metallacycle structures. The distance between the two C atoms which will form the new C−C bond was assumed as the reaction coordinate. At each point, the C−C distance assumed as the reaction coordinate was kept fixed while all the other degrees of freedom were fully optimized. To ensure that the minimum path was effectively tracked, the linear transit paths were also scanned from the products to the reactants.

Full transition-state searches were started from the structures corresponding to the maximum of the energy along the linear transit paths. The real nature of these structures as first-order saddle points was confirmed by frequency calculations which resulted in only one imaginary frequence. To save computer time, in the frequency calculations (and only at this stage) the aromatic ring of the alkylidene and the spectator $PCy_3$, IMes, $IMesH_2$, and $(t\text{-Bu})_2P(CH_2)P(t\text{-Bu})_2$ ligands were frozen, with exclusion of the atoms which coordinate to the metal.

Solvent effects were considered by correcting the gas-phase energy with the use of the conductor-like screening model, COSMO, of Klamt and Schüürmann,[56] as implemented in the ADF package.[57] The calculations of the solvation energy were performed with the dielectric constants $\epsilon$ set to 2.74 to simulate toluene, the solvent experimentally used by Grubbs and co-workers,[30] and to 8.93 to represent $CH_2Cl_2$ as a solvent of higher polarity. The van der Waals surface was used to build the cavity containing the molecule, and the standard radii of (H) 1.29, (C) 2.00, (N) 1.83, (P) 2.10, and (Cl) 2.31 Å of Klamt and Schüürmann were used.[56] For Ru, we used a radius of 2.30 Å. The calculations of energies including solvation effects were performed as single-point calculations on the gas-phase optimized geometries. The 2000.01 release of the ADF package was used for these calculations.[58]

## Results

The structures of the (pre)catalysts are reported in Figure 1.[59] All the complexes assume a distorted square-pyramidal geom-


(32) Meier, R. J.; Aagaard, O. M.; Buda, F. *J. Mol. Catal. A* **2000**, *160*, 189.
(33) Ziegler, T. *Chem. Rev.* **1991**, *91*, 651.
(34) Margl, P. M.; Ziegler, T. *Organometallics* **1996**, *15*, 5519.
(35) Margl, P. M.; Ziegler, T. *J. Am. Chem. Soc.* **1996**, *118*, 7337.
(36) Lohrenz, J. C. W.; Woo, T. K.; Ziegler, T. *J. Am. Chem. Soc.* **1995**, *117*, 12793.
(37) Woo, T. K.; Margl, P. M.; Lohrenz, J. C. W.; Blöchl, P. E.; Ziegler, T. *J. Am. Chem. Soc.* **1996**, *118*, 13021.
(38) Margl, P. M.; Deng, L.; Ziegler, T. *J. Am. Chem. Soc.* **1998**, *120*, 5517.
(39) Guerra, G.; Longo, P.; Corradini, P.; Cavallo, L. *J. Am. Chem. Soc.* **1999**, *121*, 8651.
(40) Deng, L.; Woo, T. K.; Cavallo, L.; Margl, P. M.; Ziegler, T. *J. Am. Chem. Soc.* **1997**, *119*, 6177.
(41) Deng, L.; Margl, P.; Ziegler, T. *J. Am. Chem. Soc.* **1999**, *121*, 6479.
(42) Versluis, L.; Ziegler, T. *J. Am. Chem. Soc.* **1989**, *111*, 2018.
(43) Ziegler, T.; Versluis, L.; Tschinke, V. *J. Am. Chem. Soc.* **1986**, *108*, 612.
(44) Cheong, M.; Schmid, R.; Ziegler, T. *Organometallics* **2000**, *19*, 1973.
(45) Cavallo, L.; Solà, M. *J. Am. Chem. Soc.* **2001**, *123*, 12294.
(46) Cavallo, L.; Jacobsen, H. *Angew. Chem., Int. Ed.* **2000**, *39*, 589.
(47) Jacobsen, H.; Cavallo, L. *Chem. Eur. J.* **2001**, *7*, 800.
(48) *ADF 2.3.0, User's Manual*; Vrije Universiteit Amsterdam: Amsterdam, The Netherlands, 1996.
(49) Baerends, E. J.; Ellis, D. E.; Ros, P. *Chem. Phys.* **1973**, *2*, 41.
(50) te Velde, G.; Baerends, E. J. *J. Comput. Phys.* **1992**, *99*, 84.
(51) te Velde, G.; Bickelhaupt, F. M.; Baerends, E. J.; Fonseca Guerra, C.; Van Gisbergen, S. J. A.; Snijders, J. G.; Ziegler, T. *J. Comput. Chem.* **2001**, *22*, 931.
(52) Vosko, S. H.; Wilk, L.; Nusair, M. *Can. J. Phys.* **1980**, *58*, 1200.
(53) Becke, A. *Phys. Rev. A* **1988**, *38*, 3098.
(54) Perdew, J. P. *Phys. Rev. B* **1986**, *33*, 8822.
(55) Perdew, J. P. *Phys. Rev. B* **1986**, *34*, 7406.
(56) Klamt, A.; Schüürmann, G. *J. Chem. Soc., Perkin Trans. 2* **1993**, 799.
(57) Pye, C. C.; Ziegler, T. *Theor. Chem. Acc.* **1999**, *101*, 396.
(58) *ADF 2000.02, User's Manual*; Vrije Universiteit Amsterdam: Amsterdam, The Netherlands, 2000.

(59) To save space, only the most important structures will be sketched in the following. However, the complete set of coordinates and energies is reported in the Supporting Information.

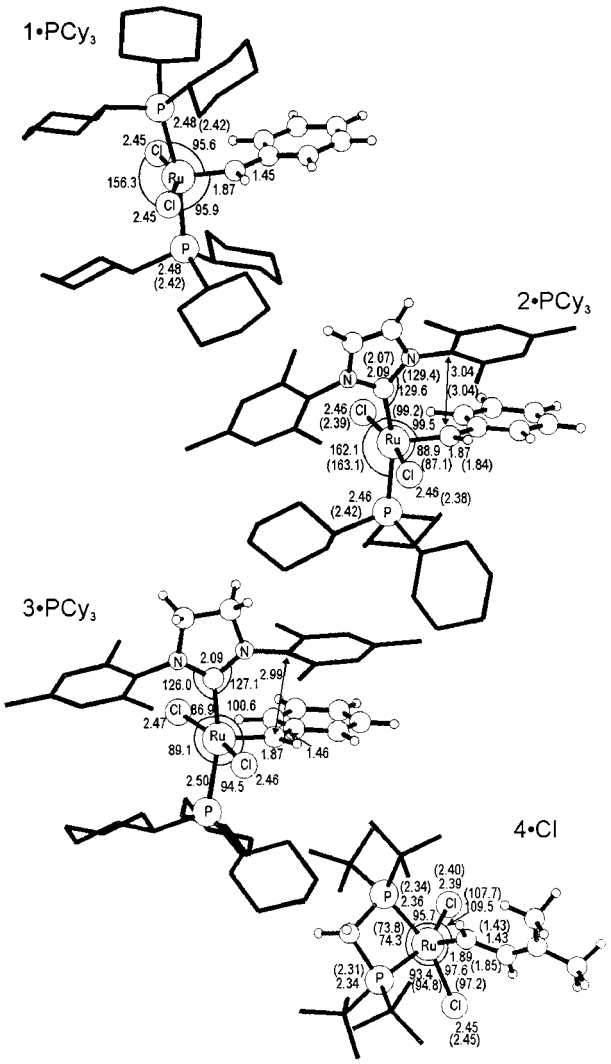


***Figure 1.*** DFT optimized structures of the various (pre)catalysts. Distances and angles are reported in Å and deg, respectively. In the case of the **1**·$PCy_3$, **2**·$PCy_3$, and **4**·Cl (pre)catalysts, the bracketed values correspond to the values found in the corresponding crystalline structure, reported in refs 30, 7, and 11, respectively.

etry with the alkylidene group at the vertex. In the **1**- to **3**-based structures the phenyl group of the Ru=CHPh moiety is almost coplanar with the Cl atoms. In the **4**-based structure, instead, the Ru=CH−$CHMe_2$ moiety does not bisect the Cl−Ru−Cl plane, but is rotated toward one of the Cl atoms as in the X-ray structure.[11] The smallest Cl−Ru=C−C torsional angle we calculated is equal to 27°, to be compared to the value of 22° in the crystalline structure. Of interest is the deviation from planarity around the *ipso*-C atom of the mesityl groups in the **2**- and **3**-based structures. In fact, while the angle N−C(*ipso*)−C(*para*) should be equal to 180°, they are close to 175° in **2**·$PCy_3$ and to 173° in both **3**·$PCy_3$ and **3**·$PPh_3$. This deviation, roughly 2°, occurs also in the X-ray structure of **2**·$PCy_3$.[7] In all cases, the deviation pulls the mesityl groups away from the Cl and alkylidene ligands. Finally, it is worthy to note that steric interactions between the mesityl groups and the Cl atoms keep the NHC ring coplanar with the Ru=C(alkylidene) bond. In fact, in the **2QM**-based structures, where the mesityl groups are absent, the NHC ring rotates considerably around the Ru−C axis, and in the same cases it was almost coplanar with the Ru−Cl bonds.

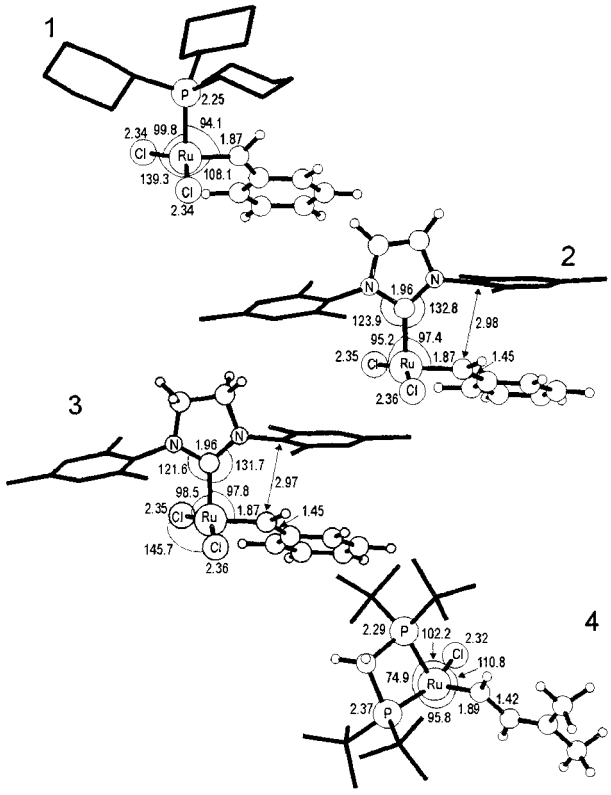


***Figure 2.*** DFT optimized structures of the ethene free intermediates. Distances and angles are reported in Å and deg, respectively.

The geometries reported in Figure 1 also indicate that the BP86 functional reproduces well the X-ray geometries of **2**·$PCy_3$ and **4**·Cl. The root-mean-square deviation of the calculated geometries from the X-ray structures is equal to 0.07 Å for both **2**·$PCy_3$ and **4**·Cl. With respect to the Ru−X distances, the calculated values slightly overestimate the corresponding experimental distances. Inclusion of relativistic effects in the geometry optimization would reduce the Ru−X distances,[60] thus leading to a better agreement with the experimental values.

The structures of the phosphine-free intermediates **1**−**3** and of the cationic **4** species after dissociation of $Cl^-$ are reported in Figure 2. The removal of one of the ligands scarcely modifies the overall geometry of the remaining ligands, although all the distances of coordination from the Ru atom are shortened as a consequence of the reduced electron density at the metal. Moreover, in **1**, **2**, and **3** the phenyl group of the Ru=CHPh moiety rotates by roughly 30−40° toward the coordination position previously occupied by the phosphine. This finding is in agreement with the crystal structure of $(PCy_3)(t\text{BuO})_2$Ru=CHPh, in which the =CHPh group is almost perpendicular to the O−Ru−O plane,[61] and with previous theoretical calculations which indicated a very facile rotation of the alkylidene around the Ru=C bond.[23,26] In the case of **2** and **3** a very short distance, below 3.0 Å, occurs between the C atom of the alkylidene bound to the metal and the *ipso*-C atom of the above mesityl ring, a consequence of the shrinking of the Ru−C(NHC) distance. To relieve these steric interactions, the mesityl groups in **2** and **3** bend away from the alkylidene, and the N−C(*ipso*)−C(*para*)

(60) Jacobsen, H.; Schreckenbach, G.; Ziegler, T. *J. Phys. Chem.* **1994**, *98*, 11406.
(61) Sanford, M. S.; Henling, L. M.; Day, M. W.; Grubbs, R. H. *Angew. Chem., Int. Ed.* **2000**, *39*, 3451.

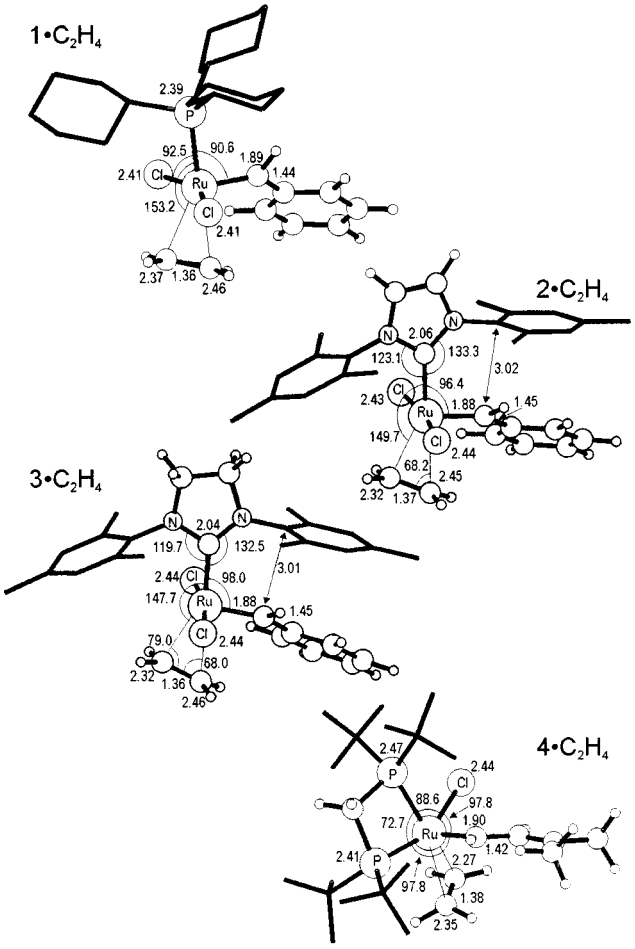


***Figure 3.*** DFT optimized structures of the ethene bound intermediates **1**·$C_2H_4$, **2**·$C_2H_4$, **3**·$C_2H_4$, and **4**·$C_2H_4$. Distances and angles are reported in Å and deg, respectively.

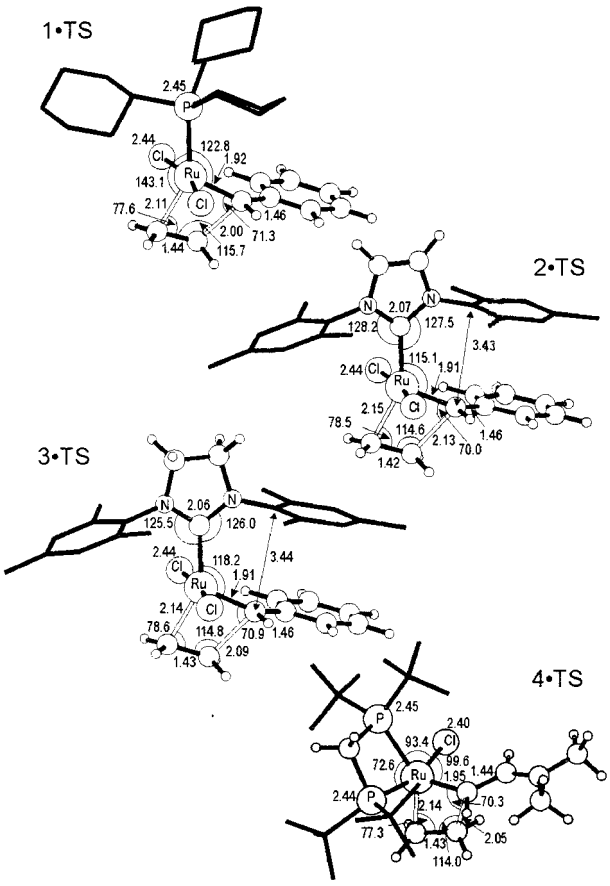


***Figure 4.*** DFT transition states for ethene insertion into the Ru=C bond of the ethene bound intermediates **1**·$C_2H_4$, **2**·$C_2H_4$, **3**·$C_2H_4$, and **4**·$C_2H_4$. Distances and angles are reported in Å and deg, respectively.

angles in both **2** and **3** are now close to 175°. Also the NHC ring bends away from the alkylidene, as indicated by the larger value we calculated in **2** and **3** for the Ru−C−C angle near the alkylidene, ∼130 °C, relative to the value of ∼125° assumed by the Ru−C−N angle opposite the alkylidene.

Ethene coordination leads to the ethene-bound intermediates of Figure 3. Test calculations on ethene coordination to the simple $PH_3Cl_2Ru{=}CH_2$ model suggested the absence of an enthalpic barrier to olefin coordination. Of course, unfavorable entropic effects could give rise to a free energy barrier to olefin coordination. This aspect would require an ab initio molecular dynamic study such as that performed by Woo and Ziegler on the free-energy barrier of ethene coordination to a Ni(II) complex.[62] However, such a study is out of the scope of the present paper.

Ethene coordination restores the square-pyramidal geometry in all cases. In the **1**·$C_2H_4$, **2**·$C_2H_4$, and **3**·$C_2H_4$ intermediates the C=C double bond of the olefin is almost parallel to the Ru=C(alkylidene) bond. However, we also tried different geometries in which the C=C double bond is roughly perpendicular to the Ru=C(alkylidene) bond, since in previous theoretical studies this geometry was found to be the most stable for the simple $PH_3Cl_2Ru{=}CH_2(C_2H_4)$ model.[23,26] We found this situation to be of marginally higher energy. In the case of the simple $PH_3Cl_2Ru{=}CH_2(C_2H_4)$ model, the minimum energy BP86 geometry is in agreement with the previous studies since it predicts the structure with the C=C double bond almost perpendicular to the Ru=C bond as the most stable.

In all the ethene-bound intermediates the olefin is unsymmetrically coordinated, while the C=C bond is slightly elongated from the value assumed in the free $C_2H_4$ molecule (1.34 Å). The geometries of Figure 3 also indicate that in case of the NHC based **2**·$C_2H_4$ and **3**·$C_2H_4$ intermediates the olefin is more tightly bound to the metal relative to the **1**·$C_2H_4$ intermediate, since the Ru−C(olefin) distances are slightly shorter in **2**·$C_2H_4$ and **3**·$C_2H_4$ relative to **1**·$C_2H_4$. The shortest Ru−C(olefin) distances are predicted for **4**·$C_2H_4$, which is reasonable considering its cationic character. Interestingly, in the last structure the olefin is almost perpendicular to the Ru=C bond. Finally, ethene coordination relaxes a little the steric strain between one of the mesityl rings and the alkylidene moiety in **2**·$C_2H_4$ and **3**·$C_2H_4$, since the shortest distance of interaction between these groups is now just above 3.0 Å. The relax is due to longer distances of coordination of the NHC ligands upon ethene coordination. Other evidence is given by the angles N−C(*ipso*)−C(*para*) which are close to 178° in both **2**·$C_2H_4$ and **3**·$C_2H_4$.

The transition states for ethene insertion into the Ru=C bond are reported in Figure 4. The reacting atoms assume an almost planar four-center geometry, which is typical for olefin insertion into Mt−C $\sigma$-bonds.[36,40,63−65] The deviation of the C atom of

(62) Woo, T. K.; Blöchl, P. E.; Ziegler, T. *J. Phys. Chem. A* **2000**, *104*, 121.

(63) Lauher, J. W.; Hoffmann, R. *J. Am. Chem. Soc.* **1976**, *98*, 1729.

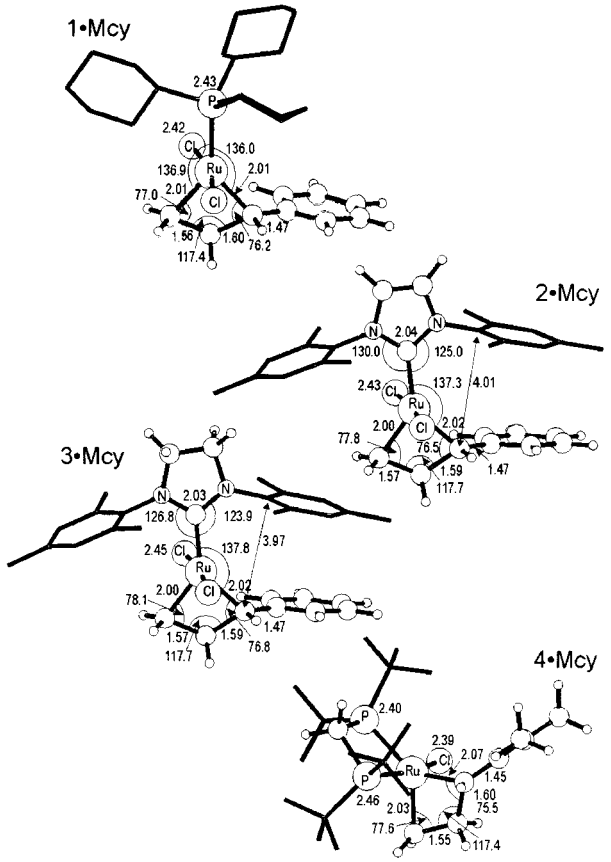


***Figure 5.*** DFT optimized structures of the metallacycles **1**·Mcy, **2**·Mcy, **3**·Mcy, and **4**·Mcy. Distances and angles are reported in Å and deg, respectively.

the olefin which is going to form the new C−C bond from the plane defined by the forming C−Ru−C single bonds is smaller than 0.4 Å. The Ru═C(alkylidene) bond bends toward the olefin by roughly 20°, whereas the overall position of the two olefinic C atoms is substantially unmodified, except for an obvious shortening of the metal−olefin distance of the incipient Ru−C bond. In the case of the **4**·TS structure, the olefin rotates in a concerted way with the bending of the Ru═C group, to facilitate the formation of the new C−C bond. As for the other ligands, it is remarkable the noticeable elongation (almost 0.1 Å) of the Ru−P bond in **1**·TS. A similar elongation of the Ru−N distance is not observed in the case of the NHC-based **2**·TS and **3**·TS species. In **1**·TS this effect can be ascribed to the trans effect of the two incipient Ru−C $\sigma$-bonds on the soft $PCy_3$ ligand. For the NHC-based transition states, the bending of the alkylidene toward the olefin reduces the steric stress between the alkylidene and the nearby mesityl group. The shortest distance between these two groups is now close to 3.4 Å.

The geometries of the metallacycle products which have been obtained by full optimization of the structures corresponding to the last point of the linear transit paths are reported in Figure 5. In all the structures the metallacycle is almost planar. As a measure of the puckering, the deviation of the C atom opposite to the Ru atom from the C−Ru−C plane is smaller than 0.5 Å. As for the transition states, the greatest deviation occurs for the **4**-based structure. Moreover, in **1**·Mcy, **2**·Mcy, and **3**·Mcy

***Table 1.*** Binding Energies, in kcal/mol, of the Various Ligands in the (Pre)catalysts and of the Ethene in the Olefin-Bound Intermediates[a]

| | | $\Delta G_s$ | |
|---|---|---|---|
| | gas-phase $\Delta E_g$ | $\epsilon = 2.74$ | $\epsilon = 8.93$ |
| **1**·IMes | 39.5 | 39.0 | 26.7 |
| **1**·$IMesH_2$ | 34.6 | 29.3 | 21.1 |
| **1**·$PCy_3$ | 16.2 | 14.1 | 13.3 |
| **1**·$C_2H_4$ | 6.2 | 5.6 | 5.9 |
| **1a**·$PCy_3$ | 14.3 | 13.4 | 11.6 |
| **1a**·$C_2H_4$ | 5.4 | 5.2 | 5.1 |
| **1QM**·$PCy_3$ | 23.7 | 22.6 | 21.6 |
| **1QM**·$C_2H_4$ | 11.5 | 11.0 | 10.7 |
| **2**·$PCy_3$ | 28.2 | 26.3 | 25.2 |
| **2**·$C_2H_4$ | 14.2 | 13.7 | 12.8 |
| **2QM**·$PCy_3$ | 15.1 | 15.9 | 12.9 |
| **2QM**·$C_2H_4$ | 11.9 | 10.6 | 11.7 |
| **3**·$PCy_3$ | 23.0 | 21.5 | 20.6 |
| **3**·$PPh_3$ | 20.4 | 19.5 | 21.4 |
| **3**·$C_2H_4$ | 14.7 | 14.4 | 14.2 |
| **4**·$C_2H_4$ | 9.3 | 8.1 | 8.5 |
| **4QM**·$C_2H_4$ | 19.0 | 18.3 | 18.0 |

[a] The solvent-phase binding energies were obtained by inclusion of solvent effects with the COSMO model. The Dielectric constants of $\epsilon = 2.74$ and 8.93 were used to simulate toluene and $CH_2Cl_2$ as solvent, respectively.

the Cl−Ru−Cl angle is closer to 180° relative to the (pre)-catalyst and ethene-bound intermediates, and the three atoms form an axis that almost bisects the metallacycle ring. The former R═C bond, which evolved into a Ru−C single bond, is only ∼0.15 Å longer in the metallacycles relative to the ethene-bound intermediates. The Ru−P distance is longer by 0.05 Å in **1**·Mcy and **1a**·Mcy relative to the corresponding ethene-bound intermediates, whereas the Ru−N distances in **2**·Mcy and **3**·Mcy are slightly shorter relative to **2**·$C_2H_4$ and **3**·$C_2H_4$. Finally, the angles N−C(*ipso*)−C(*para*) are now close to the ideal value, 180°, in both **2**·Mcy and **3**·Mcy.

## Discussion

With regard to energetics, the gas phase, $\Delta E_g$, and solution free energy, $\Delta G_s$, of binding of $PPh_3$, $PCy_3$, and $C_2H_4$ to **1**−**4** are reported in Table 1.

The binding energies we calculated for **1**·$PCy_3$, **1a**·$PCy_3$, **2**·$PCy_3$, **3**·$PCy_3$, and **3**·$PPh_3$ (16.2, 14.3, 28.2, 23.0, and 20.4 kcal/mol, respectively) can be compared to the corresponding phosphine exchange activation $\Delta H^{\ddagger}$ (23.6 ± 0.5, 24 ± 1, 25 ± 4, 27 ± 2, and 21 ± 3 kcal/mol, respectively) measured by Grubbs.[30] The binding energies we calculated show a reasonable correlation with the experimental activation energies. However, it must be noted that the experimental numbers are activation $\Delta H^{\ddagger}$, while our numbers are binding energies. The ab initio molecular dynamic study performed by Woo and Ziegler on the free-energy barrier of ethene coordination to a Ni(II) complex [62] showed that zero point vibrational energies ($\Delta H_{ZPE}$,) and thermodynamic components ($\Delta H_{rot}$, $\Delta H_{trans}$, and $\Delta H_{vib}$) can contribute with 3−4 kcal/mol to the overall $\Delta H^{\ddagger}$. For this reason, we think it is reasonable that our numbers, either $\Delta E_g$ or $\Delta G_s$, are usually lower than the experimental $\Delta H^{\ddagger}$, although in the case of **1a**·$PCy_3$ the calculated binding energies are probably too low. An overall better agreement is obtained if the calculated binding energies are compared to the experimental phosphine exchange $\Delta G^{\ddagger}$ (19.9 ± 0.1, 22.0 ± 0.2, 24 ± 1, 23.0 ± 0.4, and 19.6 ± 0.3 kcal/mol, respectively). The $\Delta E_g$ we calculated for **1QM** and **2QM** are in good agreement with the values that Herrmann and co-workers calculated for rather similar model systems.[8]

(64) Kawamura-Kuribayashi, H.; Koga, N.; Morokuma, K. *J. Am. Chem. Soc.* **1992**, *114*, 8687.
(65) Yoshida, T.; Koga, N.; Morokuma, K. *Organometallics* **1995**, *14*, 746.

As regards a comparison between phosphines and the NHC ligands (entries **1**·$PCy_3$, **1**·IMes, and **1**·$IMesH_2$in Table 1), the NHC ligands coordinate more strongly to Ru than $PCy_3$ by roughly 20 kcal/mol in the gas phase. The higher binding energy of the NHC ligands relative to the $PCy_3$ ligand is in agreement with calorimetric data,[7] and with previous density functional theory calculations.[8] This value is reduced to roughly 8−10 kcal/mol when solvent effects are considered, in better agreement with the values obtained by solution calorimetry data on systems of the type $Cp^*Ru(L)Cl$ (L = $P^iPr_3$, $PCy_3$, IMes), which proved that the IMes ligand is a stronger binder to the CP*RuCl fragment, relative to $PCy_3$, by 5 kcal/mol.[7]

With regard to olefin coordination, the calculated energetics of ethene binding follow the same trend calculated for phosphines. That is, ethene is more prone to coordinate to the NHC-based systems **2** and **3** than to the first-generation Grubbs systems **1** and **1a**. The binding $\Delta E_g$ and $\Delta G_s$ values of ethene to **1**, **1a**, and **4** are quite low, about 5−10 kcal/mol, and inclusion of unfavorable entropic factors further decreases the probability of formation of **1**·$C_2H_4$, **1a**·$C_2H_4$, and **4**·$C_2H_4$ as reactive intermediates. Differently, the $\Delta E_g$ and $\Delta G_s$ values of ethene to **2** and **3**, ∼15 kcal/mol, are noticeably high and inclusion of entropic factors should not prevent the formation of **2**·$C_2H_4$ and **3**·$C_2H_4$.

Coordination of the phosphines is always favored with respect to ethene coordination, but this energy preference depends on the system considered. In particular, the difference between the calculated binding energies of $PCy_3$ and ethene to **1**, **1a**, **2**, and **3** and of $PPh_3$ and ethene to **3** are 10.0, 8.9, 14.0, 8.3, and 5.7 kcal/mol in favor of phosphine coordination, respectively. These numbers can be related to the ratio between the rates of phosphine and of olefin coordination to the naked intermediate **II** of Scheme 2, which Grubbs and co-workers showed to be relevant to understanding the relative activity of these systems. With the exception of **2**, the energy differences we calculated are in good qualitative agreement with the trend experimentally found for the activity of these systems.[30]

The better binding properties of **2** versus **3** can be ascribed to the relative stability of the lone-pair carbenic HOMO of the IMes and $IMesH_2$ ligands. In fact, the HOMO of IMes is roughly 0.15 eV more stable than the HOMO of $IMesH_2$, which results in a weaker trans effect of IMes relative to $IMesH_2$.[66]

Solvent effects reduce the absolute binding energies of the phosphines and of the NHC ligands, in agreement with the experimental observation that higher initiation rates were observed for the more polar solvents. As noticed by Grubbs, solvent effects can be easily rationalized in terms of the polarity of the different species. For instance, the dipole moments of **2** and $PCy_3$ are equal to 5.3 and 1.3 D, respectively. Upon $PCy_3$ coordination the dipole moment of **2**·$PCy_3$ is equal to 1.0 D only, roughly 20% of that of **2**. Importantly, solvent effects are less significant for coordination of the apolar ethene. In fact, the dipole moment of **2**·$C_2H_4$ is equal to 3.5 D, roughly 65% of that of **2**. In short, polar solvents decrease both phosphine and olefin binding energies, but the reduction is larger in the case of the phosphines, and this results in smaller preference for phosphine coordination and, consequently, higher initiation rates. Of course, the higher the polarity of the solvent the higher the effect (compare entries for $CH_2Cl_2$, $\epsilon$ = 8.93, with those for toluene, $\epsilon$ = 2.74).

(66) A discussion about the physical meaning and suitability of DFT molecular orbitals for this type of analysis can be found in refs 67 and 68.

***Table 2.*** Relative Energies, in kcal/mol, of the Structures along the Reaction Path Corresponding to Ethene Insertion into the Ru=C Bond[a]

| | | $\Delta G_s$ | |
|---|---|---|---|
| | gas-phase $\Delta E_g$ | $\epsilon$ = 2.74 | $\epsilon$ = 8.93 |
| **1**·$C_2H_4$ | 0.0 | 0.0 | 0.0 |
| **1**·TS | 8.2 | 7.7 | 7.5 |
| **1**·Mcy | 5.4 | 4.5 | 4.1 |
| **1a**·$C_2H_4$ | 0.0 | 0.0 | 0.0 |
| **1a**·TS | 7.5 | 7.3 | 7.2 |
| **1a**·Mcy | 3.9 | 3.8 | 3.9 |
| **1QM**·$C_2H_4$ | 0.0 | 0.0 | 0.0 |
| **1QM**·TS | 12.0 | 11.3 | 10.8 |
| **1QM**·Mcy | 6.4 | 5.6 | 5.1 |
| **2**·$C_2H_4$ | 0.0 | 0.0 | 0.0 |
| **2**·TS | 1.9 | 2.1 | 2.4 |
| **2**·Mcy | −2.9 | −2.8 | −2.7 |
| **2QM**·$C_2H_4$ | 0.0 | 0.0 | 0.0 |
| **2QM**·TS | 8.9 | 8.4 | 8.1 |
| **2QM**·Mcy | 1.7 | 1.0 | 0.8 |
| **3**·$C_2H_4$ | 0.0 | 0.0 | 0.0 |
| **3**·TS | 1.9 | 1.8 | 2.0 |
| **3**·Mcy | −3.1 | −2.9 | −3.0 |
| **4**·$C_2H_4$ | 0.0 | 0.0 | 0.0 |
| **4**·TS | 7.9 | 8.1 | 8.4 |
| **4**·Mcy | 2.9 | 3.1 | 3.4 |
| **4QM**·$C_2H_4$ | 0.0 | 0.0 | 0.0 |
| **4QM**·TS | 8.3 | 8.7 | 9.1 |
| **4QM**·Mcy | 4.1 | 4.5 | 4.6 |

[a] For all the systems, the ethene bound intermediate is assumed as the reference state at zero energy. The solvent-phase binding energies were obtained by inclusion of solvent effects with the COSMO model. The dielectric constants of $\epsilon$ = 2.74 and 8.93 were used to simulate toluene and $CH_2Cl_2$ as solvent, respectively

With regard to the metathesis reaction, the relative energies of the transition states and of the metallacycle products with respect to the olefin bound intermediates are reported in Table 2. We found substantially low energy barriers independently of the systems considered. Systems **1**, **1a**, and **4** have the highest barrier, 5−8 kcal/mol, depending on the particular level of theory utilized, while the two NHC-based systems **2** and **3** have barriers below 2 kcal/mol. Barriers of this height support the approximation "*that all of the steps after olefin coordination (particularly metallacyclobutane formation) are fast*", invoked by Grubbs to develop its mechanistic scheme.[30]

The rather lower barriers calculated for the NHC-based systems **2** and **3**, relative to the "classical" system **1**, are also consistent with the higher activity shown by the NHC-based systems. This suggests that the barrier of the metathesis step influences the overall reaction rate, which would depend on two key factors: a preequilibrium between the phosphine-bound and olefin-bound intermediates **I** and **III** of Scheme 1 (through the phosphine-free intermediate **II**), and an intrinsic propensity toward the metathesis reaction. Compared to the first-generation Grubbs catalysts, the NHC-based systems have slower initiation rates because of the higher energy required to dissociate the phosphine. However, as argued by Grubbs they have a higher activity because olefin coordination is competitive relative to re-binding of the phosphine. Nonetheless, our calculations clearly indicate that the higher activity of the NHC-based systems can be connected also to their substantially low energy barrier for the metathesis reaction. This helps the active species to perform more metathesis steps than the first-generation Grubbs catalysts, before being trapped back from free phosphine.

The energetics we calculated is also consistent with the experimental findings which showed that in the gas phase a Grubbs-type system such as **1a** is more active than a Hofmann-type system such as **4**.[24] In fact, the numbers reported in Tables

1 and 2 indicate that **1a** has the same scarce propensity of **4** to capture the olefin, but it has a lower metathesis insertion barrier. The energy difference between the insertion barrier of the metathesis reaction of **1a** and **4** we calculated is in reasonable agreement with the experimental data, which indicated that in the gas phase a system such as **1a** is approximately 40 times more active than a system such as **4**. Solvent effects seem to reduce the insertion barrier of **1a** and to increase that of **4**, and thus the activity of **1a** with respect to **4** should be higher in solution than in the gas phase. This is not in agreement with the experimental results which indicate that **4** is more active than **1a** in solution, but supports the conclusion of Hofmann, Chen, and co-workers that the higher activity in solution of systems such as **4** is connected to a more favorable preequilibrium between the (pre)catalysts and the real active species.[24]

Finally, our calculations for **1QM** are in relatively good agreement with the height of the metathesis insertion barrier, 10.4 kcal/mol, predicted by Chen and co-workers for the simple $(PH_3)_2Cl_2Ru{=}CH_2$ model,[23] while for the insertion barrier of **4** our value is larger than that, 2.6 kcal/mol, predicted by Hofmann and co-workers for the model system $[(\kappa^2\text{-}H_2PCH_2PH_2)ClRu{=}C_2]^+$.[31]

The energy difference between the ethene-bound intermediates and the corresponding metallacycles is always quite low. Considering that we also predicted low barriers for the metathesis reactions, our calculations are consistent with the reversibility experimentally observed in ring-opening metathesis.[23,69−72] With regard to the stability of the metallacycles, our calculations indicate that for all the species considered here the metallacycle is a minimum energy situation along the reaction path. This is in agreement with previous DFT and high-level CCSD(T) calculations on model systems.[23] Moreover, in the case of the NHC systems the metallacycles are lower in energy relative to the ethene-bound intermediates, whereas in the case of the first-generation Grubbs-type and Hofmann-type systems the metallacycles are higher in energy relative to the ethene-bound intermediates. Interestingly, Chen and co-workers suggested that the metallacycle is rather a transition state than an intermediate along the reaction path, a proposal with no theoretical support. However, all the calculations reported so far (with the inclusion of those reported in this paper) have used ethene as olefin, whereas Chen and co-workers used 1-butene and norbornene.[23] To check if the nature of the olefinic substrate could alter significantly the shape of the reaction profile, we performed additional calculations on **1QM** with 1-butene and norbornene as olefinic substrates. The metallacycle is an intermediate with both olefins, and the two structures are reported in Figure 6. In the case of 1-butene the two Ru−C bonds are both 2.02 Å long, whereas in the case of norbornene the Ru−C(norbornene) and Ru−CHPh bonds are slightly shorter and longer, respectively, than the corresponding bonds in the 1-butene metallacycle intermediate. This difference can be related to the release of steric strain in the norbornene ring.

The complete energy profile from 1-butene (norbornene)-bound reactants to the products is reported in Figure 7 and reveals differences between a simple olefin such as 1-butene and norbornene. First, coordination of norbornene is considerably less favored than coordination of 1-butene, a consequence of the steric bulkiness of norbornene with respect to 1-butene. The energy barrier leading to metallacycle formation is substantially the same (9.7 and 9.6 kcal/mol for norbornene and 1-butene, respectively), and similar to that relative to ethene insertion (10.0 kcal/mol, see Table 2). In both cases the metallacycle is a minimum-energy situation. However, in the case of 1-butene the transition states leading back to 1-butene or forward to styrene are both roughly 3.7 kcal/mol above the metallacycle. Differently, in the case of norbornene the transition state leading back to norbornene is roughly 7 kcal/mol above the metallacycle, while the transition state that opens the norbornene ring is 2.3 kcal/mol above the metallacycle. The reduced barrier relative to the case of 1-butene is clearly due to the release of steric strain in the norbornene ring, as evidenced by the substantially higher exothermicity of the reaction. Although our numbers do not support that the metallacycle is a transition state, from a kinetic point of view a barrier of this height is scarcely different from a completely downhill path.

In this final section we discuss the role of the bulky Cy, Mes, and *t*-Bu substituents in **1**, **2**, and **4**. To this end, we investigated the behavior of the model systems **1QM**, **2QM**, and **4QM** which correspond to systems **1**, **2**, and **4** after removal of the Cy, Mes,

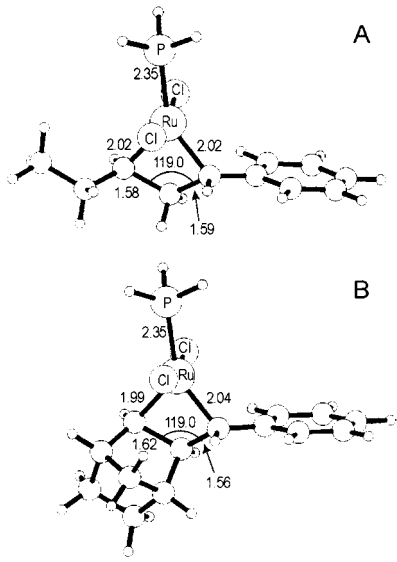


***Figure 6.*** DFT-optimized structures of the metallacycle intermediate for 1-butene (part A) and norbornene (part B) metathesis reaction with the system **1QM**. Distances and angles are reported in Å and deg, respectively.

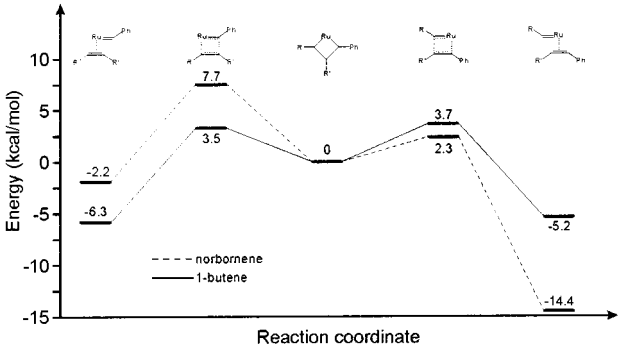


***Figure 7.*** BP86 energy profiles from olefin-coordinated reactants to products for the metathesis reaction of 1-butene or norbornene with 1QM. In both cases, the metallacycle intermediates of Figure 6 are assumed as reference structures at zero energy.

(67) Gritsenko, O.; Baerends, E. J. *J. Phys. Chem. A* **1997**, *101*, 5383.
(68) Stowasser, R.; Hoffmann, R. *J. Am. Chem. Soc.* **1999**, *121*, 3414.
(69) Marsella, N. J.; Maynard, H. D.; Grubbs, R. H. *Angew. Chem., Int. Ed. Engl.* **1997**, *36*, 1101.
(70) Lee, C. W.; Grubbs, R. H. *Org. Lett.* **2000**, *2*, 2145.
(71) Fürstner, A.; Thiel, O. R.; Ackermann, L. *Org. Lett.* **2001**, *3*, 449.
(72) Smith, A. B., III; Adams, C. M.; Kozmin, S. A. *J. Am. Chem. Soc.* **2001**, *123*, 990.

and *t*-Bu substituents from the ligands. In the case of **1**·$PCy_3$ the Cy groups were removed only from the P atom, which remains bonded to Ru during the whole metathesis reaction.

The energetics of the **1QM**-based system is rather similar to that of **1**, although the binding energies of $PCy_3$ and $C_2H_4$ to **1QM** are both larger than those to **1** by roughly 5 kcal/mol. The larger binding energies for **1QM** can be reasonably ascribed to the reduced basicity of $PH_3$ in **1QM** compared to that of $PCy_3$ in **1**, which results in a more electron deficient metal atom. Moreover, the metathesis barrier and the metallacycle product are of slightly higher energy, ∼2−3 kcal/mol, in **1QM** than in **1**, which can be connected to the better olefin-coordinating properties of **1QM** relative to **1**.

The energetics of **2QM**, instead, is remarkably different from that of **2**, since the binding energies of both $PCy_3$ and $C_2H_4$ to **2QM** are considerably lower, ∼5−10 kcal/mol, than those to the full system **2**. This result cannot be ascribed to the electronic effect of the mesityl substituents, but to their steric hindrance. As previously discussed, the mesityl groups are a short distance from the alkylidene, and this distance becomes shorter than 3.0 Å in the naked 14-electron intermediate **II**, when the Ru−NHC distance of coordination becomes shorter due to the absence of a ligand in the trans position. The steric pressure in the naked intermediate is relieved when another ligand, either a phosphine or an olefin, is coordinated and the NHC ligand is pushed away from the metal. In this framework, it is reasonable that the steric pressure of the mesityl groups in the **2**-based system lowers the metathesis reaction barrier and stabilizes the metallacycle product. In fact, the barrier of the metathesis step and the metallacycle product relative to the olefin-bound intermediate are roughly 5 kcal/mol higher in energy in the **2QM**-based system than in the **2**-based system.

These results clearly indicate the role played by the mesityl groups.[73] First, they do not promote phosphine dissociation. In fact, the phosphine and olefin free species is strongly destabilized by steric interactions between the mesityl groups and the Cl and alkylidene ligands. However, for the same reason they promote olefin coordination, which would be otherwise more labile. Finally, they also promote the following metathesis reactions and stabilize the metallacycle intermediate. Both these last effects are a consequence of the release of steric pressure as the alkylidene moves away from the NHC ligand during the metathesis reaction.

Finally, the energetics of **4QM** is also rather different from that of **4**. However, in this case the bulky *t*-Bu groups disfavor olefin coordination, since the binding energy of $C_2H_4$ to **4QM** is roughly 10 kcal/mol higher than that of $C_2H_4$ to **4**. This behavior can be connected to the steric pressure of the *t*-Bu groups on $C_2H_4$ and $Cl^-$ in **4**. Moreover, the metathesis barrier and the metallacycle product are of slightly higher energy, ∼2−3 kcal/mol, in **4QM** than in **4**, which can be connected to the better olefin-coordinating properties of **4QM** relative to **4**.

## Conclusions

In this paper we have performed a detailed quantum mechanics study of the Ru-catalyzed metathesis reaction. The main conclusions can be summarized as follows.

(1) The binding energies we calculated for coordination of phosphines to Ru in the different (pre)catalysts show a reasonable correlation with the experimental activation $\Delta H^{\ddagger}$ and $\Delta G^{\ddagger}$ of phosphine exchange. This result gives an estimation of the validity of the computational approach utilized.

(2) The binding energies we calculated for coordination of ethene to Ru in the different catalysts follow the same trend observed for the phosphines. The difference between the binding energy of the phosphines and that of the olefin depends on the catalyst considered. In particular, smaller energy differences have been calculated for the NHC-based systems. The higher propensity of the NHC-based catalysts to bind the olefin is also evidenced by the shorter Ru−olefin distances, and the longer C═C ethene bond in the olefin adducts.

(3) Solvent effects reduce the absolute binding energies of the phosphines and of the NHC ligands, whereas they scarcely modify the binding energy of the apolar ethene. This results in a smaller preference for phosphine coordination in solution and, in agreement with the experimental results, in higher initiation rates. Of course, the higher the polarity of the solvent the higher the effect.

(4) All the energy barriers we calculated for the following metathesis reaction are rather low (lower than 8 kcal/mol). However, the NHC-based systems are predicted to have a sensibly lower metathesis insertion barrier compared to the first generation of Grubbs catalysts, in qualitative agreement with their high activity.

(5) Metallacyclic structures represent minimum energy situations along the reaction coordinate, and are of slightly higher energy with respect to the corresponding olefin-bound intermediates in the case of the phosphane-based systems, while they are slightly more stable than the olefin adducts in the case of the NHC-based systems. When norbornene is considered as olefin, the energy barrier of the reaction that leads from the metallacycle to the products is only 2.3 kcal/mol.

(6) The major role played by the bulky Mes substituents in the NHC-based systems is to exert a strong steric pressure on the alkylidene moiety. This steric pressure destabilizes in a remarkable manner the phosphine and olefin free intermediate, where the Ru−NHC distance assumes its shortest value. As a consequence, *they do not promote phosphine dissociation*, and hence slow (pre)catalyst initiation. However, they also promote olefin coordination, lower the metathesis reaction barrier, and stabilize the metallacycle intermediate. For these reasons, they accelerate overall activity.

**Acknowledgment.** The author thanks L. Minieri, who contributed in the early stages of this project, and one of the reviewers for very useful comments which delayed the acceptance of the manuscript, but contributed to improve considerably the quality of this paper. This work was supported by MURST of Italy, Grant PRIN-2000, and by Basell Polyolefins. The author also thanks the CIMCF of Università Federico II of Naples for technical support.

**Supporting Information Available:** Cartesian coordinates of all the species discussed (PDF). This material is available free of charge via the Internet at http://pubs.acs.org.

JA016772S

(73) Although the main interactions occur with the *ipso*-C atom of the mesityl groups (and hence these steric effects should be present with almost any kind of substituents on the N atoms) the different bulkiness and electronics of different groups can still influence the behavior of the corresponding catalyst in a sensible way.